State-Space Representation of Unsteady Airfoil Behavior

J. G. Leishman* and K. Q. Nguyen†
University of Maryland, College Park, Maryland

A method is presented to model the unsteady lift, pitching moment, and drag acting on a two-dimensional airfoil operating under attached-flow conditions in a compressible flow. Starting from suitable generalizations and approximations to aerodynamic indicial functions, the unsteady airloads due to an arbitrary forcing are represented in a state-space (differential equation) form. This model is in a form compatible with the aeroelastic analyses of both fixed-wing and rotary-wing systems. An important feature of the method is the inclusion of the compressibility effects. The method is validated against experimentally obtained aerodynamic loads for two-dimensional airfoils undergoing oscillatory plunge, oscillatory pitch, and steady pitch rate (ramp) forcing at various Mach numbers.

Nomenclature

a = sonic velocity
A_n = coefficients of indicial functions
A_{ij} = elements of the system state matrix
b_n = exponents of indicial functions
C_{ij} = elements of the system output matrix
c = airfoil chord
C_D = pressure drag coefficient
C_M = pitching moment about the quarter-chord
C_N = normal force coefficient
C_C = chordwise force coefficient
$h(p)$ = transfer function
M = Mach number
p = Laplace variable
$\tilde{p}$ = scaled Laplace variable, $= cp/2V$
q = nondimensional pitch rate $= \dot{\alpha}c/V$
S = distance traveled in semichords $= 2/c \int_0^t V(t)\, dt$
t = time
T_I = basic noncirculatory time constant $= c/a$
u = system input
V = freestream velocity
x_i = state variable
α = angle of attack
β = compressibility factor $= \sqrt{1-M^2}$
θ = pitch angle
τ = vt/c
ϕ = indicial response function

Subscripts and Superscripts

ac = aerodynamic center
M = pitching moment about the quarter chord
q = pitch rate
x = angle of attack
C = circulatory component
I = noncirculatory (impulsive) component

I. Introduction

It is well known that accurate modeling of unsteady aerodynamics plays an important role in the aeroelastic design of both fixed-wing and rotary-wing aircraft. Since aeroelastic instabilities and flutter problems are limiting factors in the performance of nearly all aircraft, it is necessary to be able to predict these phenomena accurately during aircraft design. Since design is a lengthy iterative procedure, there is considerable incentive to be able to perform these aeroelasticity calculations quickly and inexpensively. This is especially true in the case of rotors that exhibit a complex aeroelastic behavior.

A prerequisite to any aeroelastic analysis is an accurate model for the unsteady aerodynamic behavior of the wing or airfoil section. The analyst also relies on an accurate representation of the unsteady aerodynamic forces and moments in a convenient computational form. While the unsteady aerodynamic response of an airfoil to a specific time history of forcing can now be determined with considerable detail and accuracy using computational fluid dynamic (CFD) methods,[1,2] these solutions are complex and the required computational resources are extremely large. This renders most CFD methods impractical for use in routine aeroelasticity analyses, particularly in the case of rotorcraft, and more approximate unsteady aerodynamic models must be used.

Even for two-dimensional incompressible flow, closed-form unsteady aerodynamic theories are not trivial. However, classical solutions have been obtained for the lift and pitching moment on an airfoil undergoing harmonic motion by Theodorsen[3] and Greenberg,[4] who extended Theodorsen's theory to account for a harmonically time-varying freestream velocity. Theodorsen's theory has been used widely in both fixed-wing and rotary-wing aeroelasticity. However, Theordorsen's theory has a significant deficiency since the assumption of simple harmonic motion, upon which it is based, is strictly valid only at the flutter boundary. In addtion, Theordorsen's method restricts the solution method of a rotor analysis to the frequency domain,[5] i.e., the harmonic balance method. For rotor analyses using time-marching solution techniques, the unsteady aerodynamic behavior of the blade sections must be properly modeled in the time domain.

In forward flight a helicopter rotor can encounter a variety of complex aerodynamic problems, including transonic flow on the advancing blade, dynamic stall on the retreating blade, and blade vortex interactions. All these effects are sources of time-dependent aerodynamic loads and must ultimately be accounted for in the rotor analysis. In rotary-wing aeroelasticity, approximations to the aerodynamic model are often made to simplify the overall analysis. The limiting case is a linearized, incompressible, quasisteady representation, and this approximation is used in many helicopter rotor analyses. However, the quasisteady approximation can be restrictive for rotor analysis, particularly in forward flight, where the amplitude and phasing of higher harmonic blade excitations may not be properly resolved. Thus, there is considerable current

Received April 20, 1988; revision received Dec. 20, 1988.

*Assistant Professor, Department of Aerospace Engineering. Member AIAA.

†Rotorcraft Fellow, Department of Aerospace Engineering. Student Member AIAA.

demand for unsteady aerodynamic models that can be applied in the time domain and that account for arbitrary variations of airfoil angle of attack, pitch rate, and Mach number.

One powerful approach used to obtain the airloads on an airfoil undergoing an arbitrary motion under attached flow-conditions is the indicial response method in conjuction with the superposition principle.[6] The ability to handle arbitrary forcing conditions gives this approach considerable flexibility in meeting the requirements of helicopter rotor aeroelasticity analysis. The superposition process can be performed using the well-known DuHamel integral,[6] typical applications being given in Refs. 7–9 in the form of discrete time-stepping algorithms. While these algorithms are certainly efficient, they are not always compatible with the structural equations of the lifting surface, which are in the form of differential equations. Therefore, in this paper an alternative approach is explored in which a comprehensive representation of the unsteady aerodynamic behavior of the airfoil section is expressed as a finite set of ordinary differential equations.

A fundamental part of the method is the representation of the indicial response functions themselves. Wagner[10] has obtained the indicial lift response of an airfoil operating in incompressible flow for a step change in angle of attack. However, the Wagner function has limited practical utility when the effects of compressibility are important. Also, flutter problems are more likely to occur at higher Mach numbers. Under these conditions small amplitude displacements of the airfoil section produce large changes in the airloads. The accompanying phase differences that occur between the airfoil motion and the resultant airloads are an important factor in the mechanism of flutter.

While there is no exact equivalent of the Wagner function for compressible flow, many practical difficulties in the representation of compressibility effects in the indicial response can be overcome by using certain approximations and generalizations. Such approximations for the various indicial response functions have been validated for compressible flow in a recent paper by Leishman.[11] In this paper it is shown how these indicial response functions can be readily used to formulate a state-space model for the unsteady aerodynamic behavior of a two-dimensional airfoil section operating in a compressible flow undergoing an arbitrary forcing, i.e., arbitrary variations of angle of attack and pitch rate. Initial efforts to accomplish this were described by Elliott et al.,[12] although this was performed for the lift behavior only. We should also note that the state-space representation of unsteady aerodynamic effects has been used previously by Friedmann[13] and his co-workers[14,15] for rotor aeroelasticity analysis. However, because of the lack of a suitable compressible flow theory these approaches have thus far been restricted to incompressible flow.

The main impetus for using the state-space technique is that the resulting first-order ordinary differential equations describing the unsteady aerodynamics can be appended to the structural dynamic equations governing the airfoil or blade motion. The stability of the aeroelastic system can then be obtained either by eigenanalysis or by time integration of the governing equations using standard numerical algorithms. Therefore, the overall flexibility and generality of the state-space method in representing the unsteady aerodynamics makes this approach particularly attractive for many forms of aeroelasticity analysis. To support the development of the aerodynamic theory, illustrative comparisons with experimental data are presented for the unsteady lift, pitching moment, and drag on an airfoil undergoing oscillatory pitch and plunge, and steady pitch rate changes in angle of attack.

II. Methodology

A. State-Variable Concepts

The objective of this paper is to derive a concise but comprehensive description of the unsteady aerodynamic behavior of a two-dimensional airfoil (henceforth referred to as the aerodynamic system) as a finite number of first-order differential equations. The aerodynamic system receives the time histories of angle of attack, pitch rate, and Mach number as inputs and produces the corresponding unsteady lift, pitching moment, and drag as outputs.

One of the most fundamental concepts associated with the description of any dynamical system, aerodynamic or otherwise, is the state of the system. The state describes the internal behavior of that system and is simply the information required at a given instant in time to allow the determination of the future outputs from the system given future inputs. In other words, the state of the system determines its present condition and is the set of values of an appropriately chosen set of variables describing the internal workings of the system. These variables are called the state variables and define an n-dimensional vector space $\boldsymbol{x}$ called the state space.

Following Ref. 16 or 17, a general nth-order differential system with m inputs and p outputs may be represented by n first-order differential equations

$$\dot{\mathbf{x}} = \mathbf{A}\mathbf{x} + \mathbf{B}\mathbf{u} \tag{1}$$

with the output equations

$$\mathbf{y} = \mathbf{C}\mathbf{x} + \mathbf{D}\mathbf{u} \tag{2}$$

where $\dot{x} = \mathrm{d}x/\mathrm{d}t$, $\boldsymbol{u} = u_i$, $i = 1,2,...,m$ are the system inputs, and $\boldsymbol{y} = y_i$, $i = 1,2,...,p$ are the system outputs. The states of the system are $\boldsymbol{x} = x_i$, $i = 1,2,...,n$.

B. State Equations from the Indicial Response

The state equations describing the unsteady aerodynamic system can be obtained by direct application of Laplace transforms to the indicial response. To illustrate the general form of the aerodynamic state equations, consider a general indicial lift response ϕ approximated by the two-pole exponential function

$$\phi(S) = 1.0 - A_1 \exp(-b_1 S) - A_2 \exp(-b_2 S) \tag{3}$$

The scaling conventionally adopted to generalize time produces the parameter $S = 2Vt/c$ corresponding to the relative distance traveled by the airfoil in terms of semichords. In the time domain, the indicial response can be written as

$$\phi(t) = 1.0 - A_1 \exp(-t/T_1) - A_2 \exp(-t/T_2) \tag{4}$$

where

$$T_1 = \frac{c}{2Vb_1} \quad \text{and} \quad T_2 = \frac{c}{2Vb_2}$$

Furthermore, let $\phi(0) = 0 = 1 - A_1 - A_2$; then the corresponding impulse response $h(t)$ is given by

$$h(t) = \frac{A_1}{T_1}\exp(-t/T_1) + \frac{A_2}{T_2}\exp(-t/T_2) \tag{5}$$

The Laplace transform of the impulse response, or transfer function, can be rearranged to yield

$$h(\tilde{p}) = \frac{(A_1 b_1 + A_2 b_2)\tilde{p} + b_1 b_2}{\tilde{p}^2 + (b_1 + b_2)\tilde{p} + b_1 b_2}$$

From this transfer function, the lift response to an input $\alpha(t)$ can then be written in the state-space form as

$$\begin{bmatrix} \dot{x}_1 \\ \dot{x}_2 \end{bmatrix} = \left(\frac{2V}{c}\right)\begin{bmatrix} -b_1 & 0 \\ 0 & -b_2 \end{bmatrix}\begin{bmatrix} x_1 \\ x_2 \end{bmatrix} + \begin{bmatrix} 1 \\ 1 \end{bmatrix}\alpha(t) \tag{6}$$

and the output equation for the normal force coefficient are given by

$$C_N(t) = 2\pi\left(\frac{2V}{c}\right)[A_1 b_1 \;\; A_2 b_2]\begin{bmatrix} x_1 \\ x_2 \end{bmatrix} \tag{7}$$

with 2π as the lift-curve slope for incompressible flow. These equations are in the form of Eqs. (1) and (2), where in this case the matrix $\boldsymbol{D}$ is equal to zero. Thus, the state-space equations can be obtained if the indicial aerodynamic response is known.

C. Representation of the Indicial Response

The indicial lift response for an incompressible flow was first obtained theoretically by Wagner.[10] For compressible flow, some exact theoretical solutions are available (see, e.g., Lomax[18]), but only for a limited range of time. More recently, finite-difference solutions to the indicial response problem for compressible flow have been obtained by Ballhaus et al.[19] and Magnus.[20] It is experimentally impossible to obtain a direct solution for the indicial aerodynamic response. However, as shown by Mazelski,[21] Mazelski et al.,[22] Beddoes,[8] Dowell,[23] Leishman,[11] and others, it is possible to obtain the indicial response by relating back from experimental or computational results in the frequency domain. Under oscillatory conditions, unsteady aerodynamic data are certainly easier to obtain but must be known at sufficiently high reduced frequencies to make a numerical inversion possible. Even still, the problem remains as to how the indicial response functions can best be generalized and approximated in a form suitable for the performance of practical calculations.

Jones[24] used a two-pole exponential approximation to the Wagner function, i.e.,

$$\phi(S) = 1.0 - 0.165\exp(-0.0455S) - 0.335\exp(-0.3S) \tag{8}$$

In fact, the Wagner and Theodorsen functions are related through a Fourier transform pair.[6] Using Fourier transform methods, it can be shown that Jones's approximation can reproduce the frequency response to within a few percent accuracy of the exact Theodorsen solution.

It is also of some interest to note that the state equations previously presented by Friedmann and his co-workers[13–15] can be derived by replacing $\phi(S)$ in Eq. (3) by Jones's approximation to the Wagner function. Thus, Eq. (6) becomes

$$\begin{bmatrix} \dot{x}_1 \\ \dot{x}_2 \end{bmatrix} = \begin{bmatrix} 0 & 1 \\ -0.01375\left(\frac{2V}{c}\right)^2 & -0.3455\left(\frac{2V}{c}\right) \end{bmatrix}\begin{bmatrix} x_1 \\ x_2 \end{bmatrix} + \begin{bmatrix} 0 \\ 1 \end{bmatrix}\alpha_{3/4}(t) \tag{9}$$

with

$$C_N(t) = 2\pi\left[0.006825\left(\frac{2V}{c}\right)^2 \; 0.10805\left(\frac{2V}{c}\right)\right]\begin{bmatrix} x_1 \\ x_2 \end{bmatrix} + 0.5\alpha_{3/4}(t) \tag{10}$$

The extra term $0.5\,\alpha_{3/4}$ on the right-hand side of Eq. (10) [c.f. Eq. (7)] arises because the initial value of the Wagner function $\phi(0) = 1 - A_1 - A_2 = 0.5$. Conversely, applying a unit step input to the preceding state-space equation and setting the initial states to be zero, i.e., $\alpha_{3/4}(t) = 1$ for $t \geq 0$ and $x_1(0) = x_2(0) = 0$, the resulting response is exactly Jones's approximation to the Wagner function. In fact, it may be concluded here that the Theodorsen and Wagner functions and the state-space model are simply different representations of the "same" dynamical system and are easily related, as depicted in Fig. 1.

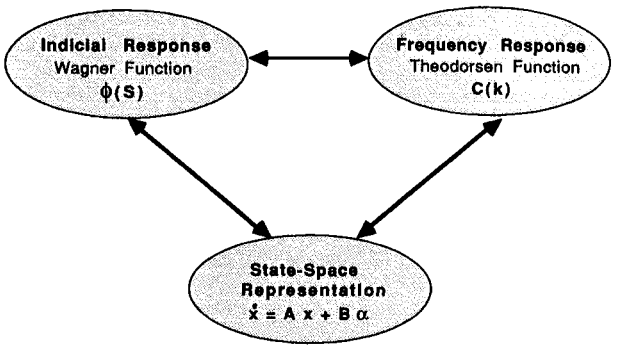

Fig. 1 Relationship between time-domain and frequency domain unsteady aerodynamics.

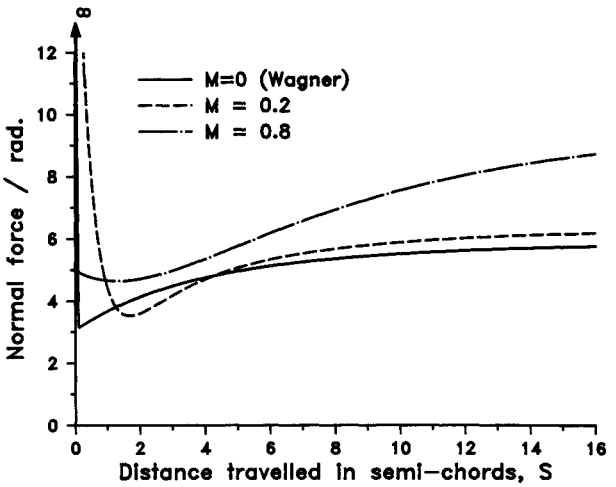

Fig. 2 Compressible vs incompressible indicial lift response to a step change in angle of attack.

Mazelski[21] appears to have been one of the first investigators to use an exponential approximation to represent the indicial response for compressible flow, where the A_j and b_j coefficients were obtained by correlating the approximate frequency-domain response with the oscillatory results of Dietze.[25] More recently, a similar approach has also been adopted by Dowell[23] to obtain approximations to the indicial response for incompressible flow using Theodorsen's result and for compressible flow using frequency response data of Williams.[26] By increasing the number of poles in Eq. (3), it is obvious that a more exact approximation to the indicial response can be made. For example, as shown by Venkatesan et al.,[27] a three-pole indicial response function can be obtained which essentially exactly reproduces the Theodorsen result over the whole frequency domain. However, a large number of poles b_j leads to an increased number of states and higher computational overheads. Furthermore, for compressible flow an increased number of coefficients can only be justfied if experimental and/or computational results of sufficient quality and range are available in the frequency domain to help validate the approximations to the indicial response functions.

In the present work, the aerodynamic indicial response functions for compressible flow are represented by up to three pole approximations. To place some physical significance on the various components, the approximation is further assumed to be idealized into two parts, as postulated by Mazelski[28] and later by Beddoes.[8] One part of the indicial response is the noncirculatory loading for which the initial value is obtained from piston theory[6] and is valid for any Mach number. For subsequent time, these initial pressure waves propagate at the local speed of sound and the loading decays

rapidly from its initial value. In fact, this noncirculatory loading may be considered as the compressible analog of the apparent mass terms used in many incompressible analyses. It can be shown that these noncirculatory terms become important contributions to the magnitude and phasing of the aerodynamic response even at relatively low reduced frequencies. The second part of the indicial response is due to the circulatory loading, which builds up quickly to the steady-state value. For the indicial lift this component is similar to the classical Küssner function.[6] The behavior of the indicial lift response for a step change in angle of attack is shown in Fig. 2 for Mach numbers of 0.3 and 0.8 in comparison with the Wagner function.

The indicial normal force and quarter chord pitching moment response to a step change in angle of attack α and a step change in pitch rate q can be written in general form as

$$\frac{C_{N_\alpha}(S)}{\alpha} = \frac{4}{M}\phi_\alpha^I(S, M) + \frac{2\pi}{\beta}\phi_\alpha^C(S, M) \tag{11}$$

$$\frac{C_{M_\alpha}(S)}{\alpha} = -\frac{1}{M}\phi_{\alpha M}^I(S, M) + \frac{2\pi}{\beta}\phi_\alpha^C(S, M)\left(\frac{1}{4} - x_{ac}(M)\right) \tag{12}$$

$$\frac{C_{N_q}(S)}{q} = \frac{1}{M}\phi_q^I(S, M) + \frac{\pi}{\beta}\phi_q^C(S, M) \tag{13}$$

$$\frac{C_{M_q}(S)}{q} = -\frac{7}{12M}\phi_{qM}^I(S, M) - \frac{\pi}{8\beta}\phi_{qM}^C(S, M) \tag{14}$$

where the indicial response functions ϕ_α^C, ϕ_α^I, $\phi_{\alpha M}^I$, ϕ_q^C, ϕ_{qM}^C, and ϕ_{qM}^I are approximated as exponential functions expressed in terms of both aerodynamic time S and Mach number M. These functions are fully defined in Ref. 11. The superscripts C and I refer to the components of circulatory and noncirculatory (impulsive) loading, respectively, and the subscript M refers to the pitching moment contribution. The second term in Eq. (12) represents the contribution to the pitching moment due to a Mach number–dependent offset of the aerodynamic center x_{ac} from the airfoil quarter-chord axis, and this parameter must be obtained from experimental airfoil data or CFD solutions. At subsonic speeds, the aerodynamic center lies close to the quarter-chord, although for transonic speeds the effective aerodynamic center moves quickly to the vicinity of the midchord as the freestream Mach number approaches unity.

D. Aerodynamic State Equations for Compressible Flow

By suitably generalizing the indicial response in terms of exponential functions and Mach number, the corresponding state equations may be obtained for each component of the loading. First, consider the normal force response to continuous forcing in terms of angle of attack. The indicial responses ϕ_α^C and ϕ_α^I due to angle of attack α are approximated for a compressible flow as[11]

$$\phi_\alpha^C(S) = 1 - A_1\exp(-b_1\beta^2 S) - A_2\exp(-b_2\beta^2 S) \tag{15}$$

and

$$\phi_\alpha^I(S) = \exp\left(\frac{-S}{T_\alpha}\right) \quad \text{or} \quad \phi_\alpha^I(t) = \exp\left(\frac{-t}{K_\alpha T_I}\right) \tag{16}$$

where the poles of the circulatory function scale with β^2. From Beddoes[8] the constants of the circulatory lift function are given as $A_1 = 0.3$, $A_2 = 0.7$, $b_1 = 0.14$, and $b_2 = 0.53$. From Leishman,[11] the noncirculatory time constant $T_\alpha = T_I K_\alpha$ is given based on an approximation to the exact linear theory results of Lomax,[18] where $T_1 = c/a$ and

$$K_\alpha(M) = [(1 - M) + \pi\beta M^2(A_1 b_1 + A_2 b_2)]^{-1}$$

The circulatory normal force response to a variation in angle of attack can be written in state-space form as

$$\begin{bmatrix}\dot{x}_1\\ \dot{x}_2\end{bmatrix} = \left(\frac{2V}{c}\right)\beta^2\begin{bmatrix}-b_1 & 0\\ 0 & -b_2\end{bmatrix}\begin{bmatrix}x_1\\ x_2\end{bmatrix} + \begin{bmatrix}1\\ 1\end{bmatrix}\alpha_{3/4}(t) \tag{17}$$

with the output equation for the normal force coefficient given by

$$C_N^C(t) = \frac{2\pi}{\beta}\left(\frac{2V}{c}\right)\beta^2[A_1 b_1 \;\; A_2 b_2]\begin{bmatrix}x_1\\ x_2\end{bmatrix} \tag{18}$$

where $2\pi/\beta$ is the lift-curve slope for linearized compressible flow and $\alpha_{3/4}$ is the angle of attack at the three-quarters-chord, i.e.,

$$\alpha_{3/4}(t) = \alpha(t) + \frac{q(t)}{2}$$

Similarly, the noncirculatory normal force due to angle of attack can be written as

$$\dot{x}_3 = \alpha(t) - \frac{1}{K_\alpha T_I}x_3 = \alpha(t) + \alpha_{33}x_3 \tag{19}$$

with the output equation for the normal force coefficient given by

$$C_{N_\alpha}^I(t) = \frac{4}{M}\dot{x}_3 \tag{20}$$

The remaining state equations for the pitching moment and pitch rate terms can be derived in a similar way and are given in the Appendix.

1. *Total Aerodynamic Response*

The individual components of aerodynamic loading are linearly combined to obtain the overall aerodynamic response. For example, the total normal force coefficient is given by

$$C_N(t) = C_N^C(t) + C_{N_\alpha}^I(t) + C_{N_q}^I(t) \tag{21}$$

and a similar equation holds for the pitching moment. Thus, the overall unsteady aerodynamic response can be described in terms of a two-input/two-output system where the inputs are the airfoil angle of attack and pitch rate and the outputs are the unsteady normal force (lift) and pitching moment. It can be readily shown that by rearranging the state equations, they can be represented in the general form

$$\dot{\mathbf{x}} = \mathbf{A}\mathbf{x} + \mathbf{B}\begin{Bmatrix}\alpha\\ q\end{Bmatrix}$$

$$\begin{Bmatrix}C_N\\ C_M\end{Bmatrix} = \mathbf{C}\mathbf{x} + \mathbf{D}\begin{Bmatrix}\alpha\\ q\end{Bmatrix}$$

where the matrices are of the form

$$\mathbf{A} = \mathbf{diag}\,[a_{11} \;\; a_{22} \;\; a_{33} \;\; a_{44} \;\; a_{55} \;\; a_{66} \;\; a_{77} \;\; a_{88}]$$

$$\mathbf{B} = \begin{bmatrix}1 & 1 & 1 & 0 & 1 & 1 & 0 & 0\\ 0.5 & 0.5 & 0 & 1 & 0 & 0 & 1 & 1\end{bmatrix}^T$$

$$\mathbf{C} = \begin{bmatrix}c_{11} & c_{21} & c_{13} & c_{14} & 0 & 0 & 0 & 0\\ c_{21} & c_{22} & 0 & 0 & c_{25} & c_{26} & c_{27} & c_{28}\end{bmatrix}$$

$$\mathbf{D} = \begin{bmatrix}4/M & 1/M\\ -1/M & -7/12M\end{bmatrix}$$

The total aerodynamic lift and pitching moment response to an arbitrary time history of α and q can be obtained from the preceding state equations by integrating numerically using a standard ordinary differential equation solver.

To illustrate this aerodynamic system more clearly, a block diagram of the state model is shown in Fig. 3. The 8×8 state matrix **A** provides a positive feedback loop in the system and essentially accounts for the time history or "memory" effects present in the aerodynamic system. These time history effects include both circulatory (shed wake) and noncirculatory (wave propagation) terms. The **D** matrix contains the initial values of the indicial response and is the "direct transmission" matrix that relates the inputs directly to the outputs while involving no system dynamics or memory effects.

2. *Unsteady Drag Force*

Referring to Fig. 4, the unsteady chord (in-plane) force and pressure drag on the airfoil may also be obtained in terms of the state variables. For a fixed-wing problem the wing has a high in-plane stiffness and so the chord force component rarely participates in the aeroelastic problem. However, for a helicopter rotor the relatively low lead/lag stiffness of the blades makes the chord force component much more significant. It can be shown that the unsteady chord force arises only from the circulatory loading on the airfoil.[29] From the output equation [Eq. (18)], the effective angle of attack of the airfoil, α_E, due to the shed wake (circulatory) terms can be written in terms of the states x_1 and x_2 as

$$\alpha_E(t) = \beta^2\left(\frac{2V}{c}\right)(A_1 b_1 x_1 + A_2 b_2 x_2) \tag{22}$$

The corresponding chord force C_C is given in terms of α_E as

$$C_C(t) = \frac{2\pi}{\beta}\alpha_E^2(t) \tag{23}$$

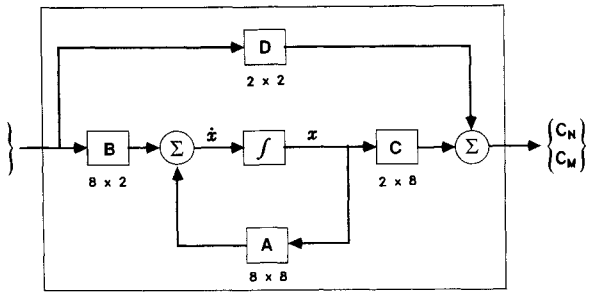

Fig. 3 Block diagram of the state model representing the unsteady aerodynamics.

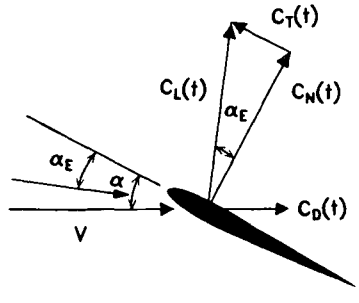

Fig. 4 Force resolution on an airfoil in unsteady flow.

which involves a bilinear combination of the states x_1 and x_2. Thus, as a byproduct of the shown system representation for the unsteady lift, the necessary information may be extracted from the system at a given instant of time to obtain the unsteady chord force component. Finally, the instantaneous pressure drag can be obtained by resolving the components of the normal force and chordwise forces through the geometric angle of attack α using

$$C_D(t) = C_N(t)\sin\alpha(t) - C_C(t)\cos\alpha(t) \tag{24}$$

Further details and validation of the unsteady chord force and pressure drag calculation are given in Ref. 29.

III. Discussion

Using the outlined state-space representation requires not only that such a formulation can be simulated accurately under arbitrary forcing but also that the linear assumption made in such a model can be suitably justified. To show this, it is necessary to consider some comparisons with experimentally obtained airfoil data. There are many good examples of unsteady airfoil behavior available in the published literature that can be used to illustrate the performance of the theory. However, in the interests of brevity in this paper, attention is confined to a few representative examples, including oscillatory plunge, oscillatory pitch, and steady pitch rate (ramp) forcing under attached-flow conditions. It should be mentioned here that for the purposes of comparison with test data the linearized value of the lift-curve slope $2\pi/\beta$ was replaced by the quasistatic value as obtained from the experimental data, as appropriate. Similarly, the aerodynamic center x_{ac} was obtained from the quasistatic test data and was implemented via Eq. (12).

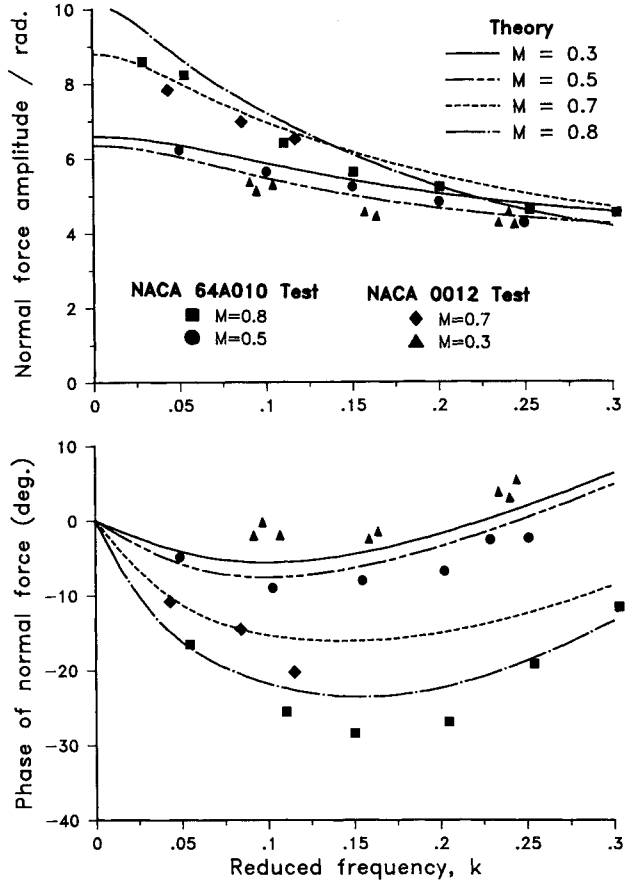

Fig. 5 Unsteady lift response to harmonic pitch oscillations.

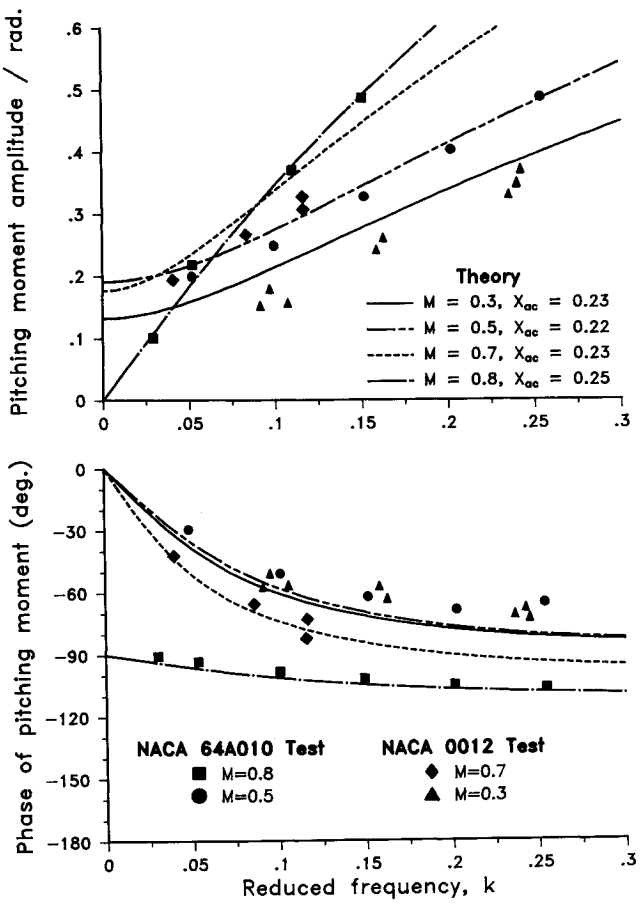

Fig. 6 Unsteady moment response to harmonic pitch oscillations.

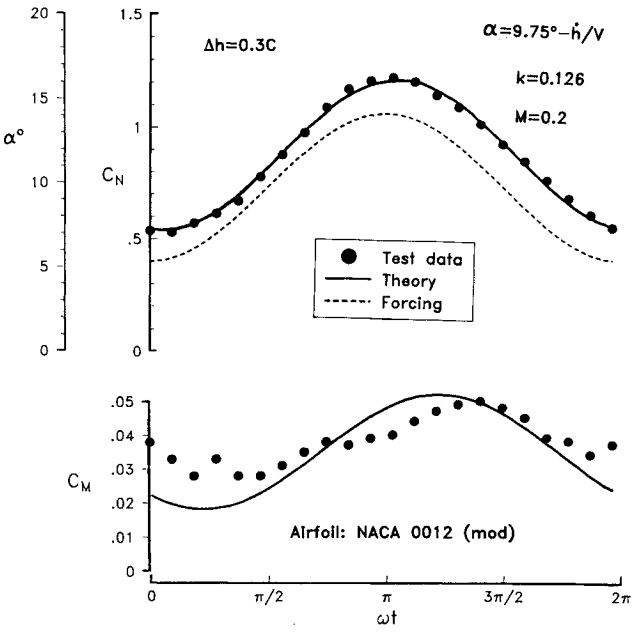

Fig. 7 Prediction of unsteady airloads on an airfoil undergoing a harmonic plunge oscillation at $M = 0.2$.

From the given state equations, the response to a particular harmonic motion can be derived in closed form. While the algebraic manipulation is somewhat lengthy, it can be shown that for a prescribed harmonic forcing explicit (exact) expressions can be obtained for the lift and moment on the airfoil as a function of forcing frequency. This provides an independent check of the aerodynamic approximations independently of any numerical integration scheme. A comparison of the (exact) theory with a selected set of lift and moment data from experiment are shown in Figs. 5 and 6 for harmonic pitch oscillations (below stall) at Mach numbers between 0.3 and 0.8. The data are presented as first harmonic amplitude and phase components vs reduced frequency. The increasing phase lag effects in the lift response with increasing Mach number are worthy of note. Also, the effects on the pitching moment amplitude and phase by moving the aerodynamic center x_{ac} in relation to the quarter-chord location should be noted.

The correlations obtained in Figs. 5 and 6 lends considerable confidence in the ability to predict accurately both the amplitude and phasing of the unsteady aerodynamic behavior due to compressibility. Furthermore, these results essentially substantiate aerodynamic linearity even for transsonic flow (i.e., the $M = 0.8$ case) as long as the flow remains attached to the airfoil, i.e., at low angles of attack. The validity of this statement has also been confirmed experimentally by Davis and Malcolm[31] from wind-tunnel tests on oscillating NACA 64A006 and 64A010 airfoils in transsonic flow.

In order to evaluate the theory using direct time integration, a computer program was developed using FORTRAN. The computer program was used to study a variety of examples of the unsteady airloads on airfoils subject to prescribed forcing below stall, and the results were correlated with experimental and computational data where available. The state equations were integrated with respect to time using a standard ordinary differential equation solver. For these particular calculations, the integration was performed using the ODE solver DE/STEP given in Ref. 32, which is a general-purpose Adams-Bashforth ODE solver with variable step size and order. Further discussion of the performance of this ODE solver is given in Ref. 33.

The first example considered is for a harmonic plunge oscillation at a Mach number of 0.2 and reduced frequency of 0.125. Plunge oscillations are of some consequence in evaluating the theory as the absence of pitch rate terms from the airloads makes it possible to evaluate the significance of the angle of attack terms independently. However, experimental plunge oscillation data are relatively unique in the published literature, mainly because of the mechanical difficulties of imparting a pure lunge motion to an airfoil. The present data have been taken from Grey and Liiva.[34]

The normal force and pitching moment coefficients for this harmonic plunge oscillation are shown in Fig. 7 and are plotted vs time. For these conditions, the normal force coefficient C_N lags the plunge displacement h by 100 deg, i.e., C_N lags the effective angle of attack $-\dot{h}/V$ by some 10 deg. This effect arises because of the lag in the buildup of the circulatory loading on the airfoil due to shed wake. On the other hand, the amplitude of the pitching moment response is due almost entirely to the noncirculatory component of aerodynamic loading on the airfoil, which has a center of pressure situated near the midchord. There is also a circulatory moment component due to an offset of the effective aerodynamic center to near 22% chord for this particular Mach number. For this plunging oscillation, the computed normal force was in excellent correlation with the test data, as shown in Fig. 7. The pitching moment response also correlated reasonably well with the test data, although there were higher harmonic components present in the test data, most likely because the airfoil was operating close to the stall and some nonlinear effects due to flow separation are inevitable.

The next example considered is for a harmonic pitch oscillation below stall. There are numerous data available in the literature for harmonically oscillating two-dimensional airfoils, and these data offer a good basis for evaluating the aerodynamic theory. For this example, the normal force, pitching moment, chord force, and pressure drag behavior are

shown for a Mach number of 0.4 and a reduced frequency of 0.075 in Fig. 8. The theory is compared with experimental data from Aircraft Research Association's (ARA) unsteady airfoil facility,[30] and these particular data have been previously published in part in Ref. 9.

These data are somewhat interesting as a significant third harmonic is present in the pitch forcing. While the amplitude of this third harmonic forcing is relatively small, the effective reduced frequency is high and would certainly be expected to contribute to the resultant airloadings. The effects of this third harmonic can be seen to a limited extent in the normal force as a distortion of what would have been a pure sinusoidal response. However, the effects are probably most discernible in the pitching moment response, where there is a significant increase in the amplitude of the higher harmonics of the pitching moment behavior due to the third harmonic of forcing. Also of interest in Fig. 8 is the behavior of the unsteady chord force. This component is rarely considered in unsteady aerodynamic models, however, it can be of some consequence in predicting the lead/lag behavior of rotor blades. As shown in Fig. 7, the theory was found to be in excellent overall agreement with all components of the airfoil loading for this example.

The next example considered is for a steady pitch rate $\dot{\theta}$ (ramp) forcing at a Mach number of 0.2. The theory is compared with test data in Fig. 9. The test data are taken from a recent experiment performed by Lorber et al.[35] The ramp motion begins at an angle of attack of zero degrees and builds up quickly to the steady-state value.

It can be seen from Fig. 9 that with increasing ramp rate there is an increasing lag in the buildup of the normal force coefficient. This lag is due mainly to circulatory effects, and the present theory was found to represent this behavior extremely well. Eventually, a fairly high angle of attack is reached and the airfoil undergoes a dynamic stall, which of course is an effect not modeled in the present work. Figure 9 shows that in the attached-flow regime the nose-down pitching moment increases with ramp rate. This effect is due mainly to noncirculatory loading components $C^I_{M_\alpha}$ and $C^I_{M_q}$ coupled with an induced camber effect C^C_{Mq}. The pressure drag is also affected by the pitch rate. As shown in Fig. 9, for a given angle of attack the pressure drag increases with increasing pitch rate. This is due to the increasing lag in the buildup of leading-edge suction (chord force component) C_C with increasing pitch rate, and hence its effect on the drag via Eq. (24).

The final example considered is a comparison of the airloads for a high-rate ramp-type change in angle of attack from 6 to 19 deg in a time period corresponding to 0.63 chord lengths of travel (i.e., $\tau = Vt/C = 0.63$). The freestream Mach number for this calculation was 0.147. This is an interesting problem that was first considered theoretically by Shamroth et al.[36] using a time-dependent Navier-Stokes solution. Later, Beddoes[8] identified the significance of the contributions made by the noncirculatory loadings during this transient motion.

A comparison of the present results with those of Shamroth are shown in Fig. 10. For the comparison, the lift and moment were computed by digitizing and integrating the pressure distributions published in Ref. 36. It should be noted that during the initial stages of the pitch motion extremely large values of lift and pitching moment are generated. This initial loading is almost entirely due to the noncirculatory terms, and the present method was found to predict both the magnitude and phasing of this transient behavior very well.

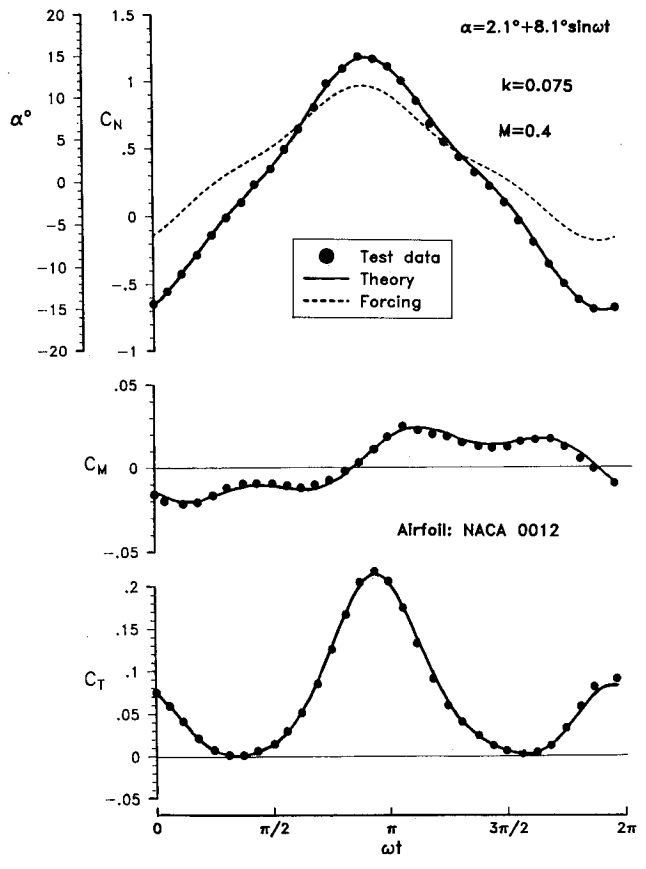

Fig. 8 Prediction of unsteady airloads on an airfoil undergoing a harmonic pitch oscillation at $M = 0.4$

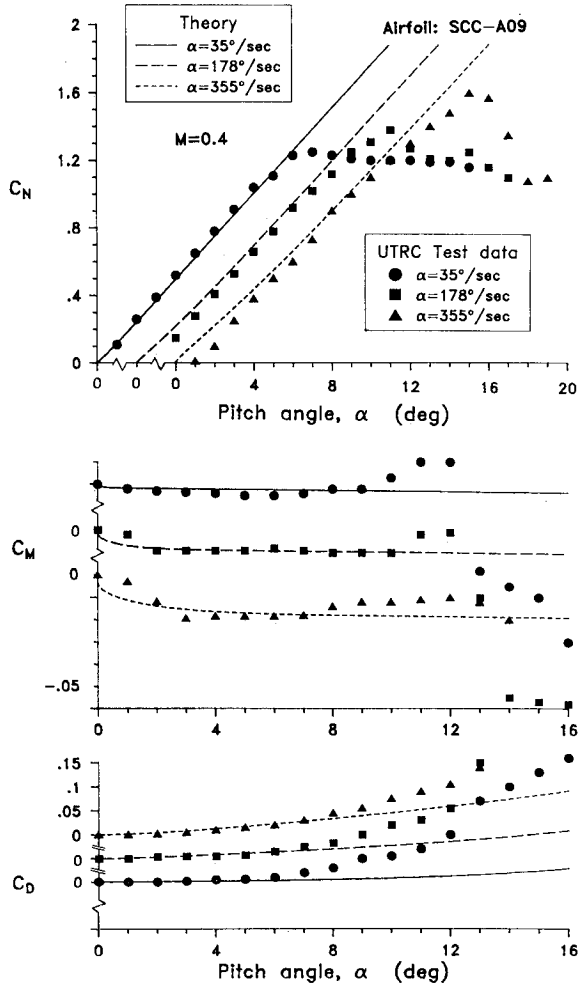

Fig. 9 Prediction of unsteady airloads on an airfoil undergoing a steady pitch rate (ramp) forcing at $M = 0.4$.

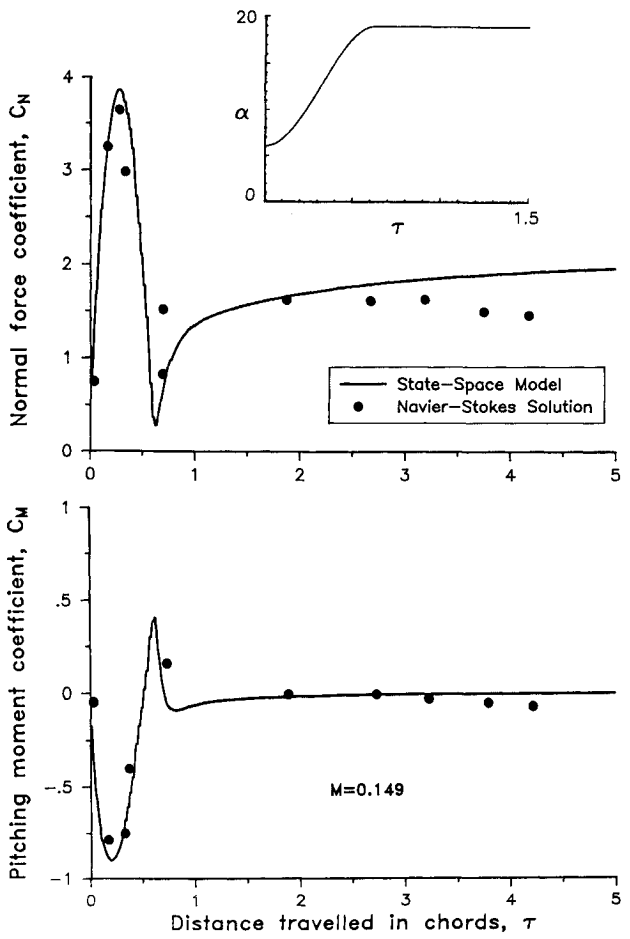

Fig. 10 Unsteady loads for high-rate ramp forcing.

At the end of the motion, the noncirculatory loading decays rapidly and the circulatory loading builds up. The airfoil finally reaches an angle of attack of 19 deg, which is above the static stall angle, and it is apparent from the Navier-Stokes calculation that some flow separation begins to develop for $\tau > 3$.

IV. Concluding Remarks

This paper describes a linearized aerodynamic method valid for arbitrary forcing in a compressible flow. Starting from approximations and generalizations for the indicial aerodynamic response, the aerodynamic lift, pitching moment, and drag response to an arbitrary forcing has been derived using state-variable techniques as a set of first-order differential equations. The main advantage of this approach is that no constraint is placed on the solution algorithm, and as such the method is useful for many forms of aeroelasticity analyses. The theory has been validated by correlating with experimental airload data on unsteady two-dimensional airfoils at various Mach numbers.

The present method has primarily addressed the *linearized* aspects of unsteady airfoil behavior. However, transsonic and viscous effects are also extremely important in rotor aeroelasticity problems, and for many flight conditions nonlinear aerodynamic prediction methods will be required, e.g., in regions of dynamic stall. Even though very sophisticated CFD methods are now becoming available that can account for such effects, these methods require very large computing resources and cannot be used routinely within helicopter rotor analysis. In fact, many rotor structural dynamic analyses are so complex that very basic aerodynamic approximations must often be used. However, with the ever increasing advances in computer technology, more sophisticated but still approximated aerodynamic methods can now be considered for these rotor analyses. The present method is designed to play such a role and in many ways bridges the gap between linearized, incompressible methods and the more comprehensive unsteady aerodynamic formulations.

Appendix A: Lift Due to Pitch Rate

The noncirculatory indicial function ϕ_q^I is defined as

$$\phi_q^I(S) = \exp\left(\frac{-S}{T_q}\right) \quad \text{or} \quad \phi_q^I(t) = \exp\left(\frac{-t}{K_q T_1}\right) \tag{A1}$$

where the noncirculatory time constant is given by

$$K_q(M) = [(1-M) + 2\pi\beta M^2(A_1 b_1 + A_2 b_2)]^{-1} \tag{A2}$$

The corresponding state-space representation can be written as

$$\dot{x}_4 = q(t) - \frac{1}{K_q T_1} x_4 = q(t) + a_{44} x_4 \tag{A3}$$

with the equation for the noncirculatory normal force due to pitch rate, $C_{N_q}^I$, given by

$$C_{N_q}^I(t) = \frac{1}{M}\dot{x}_4 \tag{A4}$$

The circulatory pitching moment due to angle of attack can be computed directly from the preceding equations if the mean aerodynamic center x_{ac} is known, and this procedure involves no additional states.

Appendix B: Moment Due to Angle of Attack

As shown in Ref. 11, a convenient general expression for the noncirculatory indicial pitching moment response due to a step change in angle of attack is of the form

$$\phi_{\alpha_M}^I(t) = A_3 \exp\left(\frac{-t}{b_3 K_{\alpha_M} T_I}\right) + A_4 \exp\left(\frac{-t}{b_4 K_{\alpha_M} T_I}\right) \tag{A5}$$

where the noncirculatory time constant is

$$K_{\alpha_M}(M) = \left[\frac{A_3 b_4 + A_4 b_3}{b_3 b_4 (1-M)}\right] \tag{A6}$$

and $A_3 = 1.5$, $A_4 = -0.5$, $b_3 = 0.25$, and $b_4 = 0.1$. The corresponding state-space equations can be written as

$$\begin{bmatrix}\dot{x}_5 \\ \dot{x}_6\end{bmatrix} = \begin{bmatrix}a_{55} & 0 \\ 0 & a_{66}\end{bmatrix}\begin{bmatrix}x_5 \\ x_6\end{bmatrix} + \begin{bmatrix}1 \\ 1\end{bmatrix}\alpha(t) \tag{A7}$$

with the output equation for the moment given by

$$C_{M_\alpha}^I(t) = \frac{-1}{M}[A_3 a_{55} \;\; A_4 a_{66}]\begin{bmatrix}x_5 \\ x_6\end{bmatrix} - \frac{1}{M}\alpha(t) \tag{A8}$$

and the elements of the state matrix given by

$$a_{55} = -(b_3 K_{\alpha_M} T_I)^{-1}, \qquad a_{66} = -(b_4 K_{\alpha_M} T_I)^{-1} \tag{A9}$$

Appendix C: Moment Due to Pitch Rate

For the circulatory indicial moment response due to a step change in pitch rate about the quarter-chord,

$$\phi_{qM}^C(S) = 1 - \exp(-b_5 \beta^2 S) \tag{A10}$$

where $b_5 = 0.5$. Finally, for the noncirculatory part,

$$\phi_{qM}^I(t) = \exp\left(\frac{-t}{K_{qM} T_I}\right) \tag{A11}$$

where the time constant is

$$K_{qM}(M) = \left[\frac{7}{15(1-M) + 3\pi\beta M^2 b_5}\right] \quad \text{(A12)}$$

The corresponding state-space equations can be written as

$$\dot{x}_7 = q(t) - b_5\beta^2\left(\frac{2V}{c}\right)x_7 = q(t) + a_{77}x_7 \quad \text{(A13)}$$

$$\dot{x}_8 = q(t) - \frac{1}{K_{qM}T_I}x_8 = q(t) + a_{88}x_8 \quad \text{(A14)}$$

with the output equations as

$$C^C_{M_q}(t) = -\frac{\pi}{8\beta}b_5\beta^2\left(\frac{2V}{c}\right)x_7 = -\frac{\pi}{16}\left(\frac{2V}{c}\right)\beta x_7 \quad \text{(A15)}$$

$$C^I_{M_q}(t) = -\frac{7}{12M}\dot{x}_8 \quad \text{(A16)}$$

It should be noted that all the indicial response functions shown are empirical approximations based on both theoretical and experimental comparisons.[11] As also shown in Ref. 11, to obtain an adequate correlation with test data, the noncirculatory constants K were reduced by 25% from their theoretical values. It should also be noted that the indicial functions described can be compared directly with those published by Bisplinghoff et al.[6]

Acknowledgments

This work was supported by the U.S. Army Research Office under the Center of Excellence for Rotary Wing Technology Program at the University of Maryland. The authors wish to acknowledge the assistance of Rotorcraft Fellow Andy Elliott (currently with McDonnell Douglas Helicopters) for his efforts in helping to establish the work contained in this paper. Also, the assistance of Rotorcraft Fellow Gilbert Crouse for programming some of the theoretical calculations is gratefully acknowledged.

References

[1]Janakiram, R. D. and Sankar, L. N., "Emerging Role of First-Principles Based Computational Aerodynamics for Rotorcraft Applications," *Proceedings of the 2nd International Conference on Rotorcraft Basic Research*, College Park, MD, 1988.

[2]McCroskey, W. J., "Some Rotorcraft Applications of Computational Fluid Dynamics," *Proceedings of the 2nd International Conference on Rotorcraft Basic Research*, College Park, MD, 1988.

[3]Theodorsen, T., "General Theory of Aerodynamic Instability and the Mechanism of Flutter," NACA Rept. 496, 1935.

[4]Greenberg, J. M., "Airfoil in Sinusoidal Motion in a Pulsating Stream," NACA TN 1326, June 1947.

[5]Friedmann, P. P. "Recent Trends in Rotary-Wing Aeroelasticity," *Vertica*, Vol. 11, No. 1/2, 1987, pp. 139–170.

[6]Bisplinghoff, R. L., Ashley, H., and Halfman, R. L., *Aeroelasticity*, Addison-Wesley, Cambridge, Mass., 1955.

[7]Beddoes, T. S., "A Synthesis of Unsteady Aerodynamic Effects Including Stall Hysteresis, *Vertica*, Vol. 1, No. 2, 1976, pp. 113–123.

[8]Beddoes, T. S., "Practical Computation of Unsteady Lift," *Vertica*, Vol. 8, No. 1, 1984, pp. 55–71.

[9]Leishman, J. G. and Beddoes, T. S., "A Generalized Model for Airfoil Unsteady Aerodynamic Behavior and Dynamic Stall Using the Indicial Method," *Proceedings of the 42nd Annual Forum of the American Helicopter Society*, Washington, DC, June 1986.

[10]Wagner, H., "Uber die Entstehung des Dynamischen Auftriesbes von Tragflugeln," *Zeitschrift für Angewandte Mathematik und Mechanic*, Vol. 5, No. 1, Feb. 1925.

[11]Leishman, J. G., "Validation of Approximate Indicial Aerodynamic Functions for Two-Dimensional Subsonic Flow," *Journal of Aircraft*, Vol. 25, Oct. 1988, pp. 914–922.

[12]Elliott, A. S., Leishman, J. G., and Chopra, I., "Rotor Aeromechanical Analysis Using a Nonlinear Aerodynamic Model," *Proceedings of the 44th Annual Forum of the American Helicopter Society*, Washington, DC, 1988.

[13]Friedmann, P. P. and Venkatesan, C., "Finite-State Modeling of Unsteady Aerodynamics and its Application to a Rotor Dynamic Problem," *Proceedings of the 11th European Rotorcraft Forum*, Amsterdam, Sept. 1985.

[14]Dinyavari, M. A. H. and Friedmann, P. P., "Unsteady Aerodynamics in Time and Frequency Domains for Finite Time Arbitrary Motion of Rotary Wings in Hover and Forward Flight," *Proceedings of AIAA/ASME/ASCE/AHS 25th Structures, Structural Dynamics and Materials Conference*, Palm Springs, CA, 1984.

[15]Dinyavari, M. A. H. and Friedmann, P. P., "Application of the Finite State Arbitrary Motion Aerodynamics to Rotor Blade Aeroelastic Response in Hover and Forward Flight," *Proceedings of AIAA/ASME/ASCE/AHS 26th Structures, Structural Dynamics and Materials Conference*, Orlando, FL, 1985.

[16]Fortmann, T. E. and Hitz, K. L., *An Introduction to Linear Control Systems*, Marcel Dekker, Inc., New York and Basel, 1977.

[17]Kailath, T., *Linear Systems*, Prentice-Hall, Englewood Cliffs, NJ, 1980.

[18]Lomax, H., Heaslet, M. A., Fuller, F. B., and Sluder, L., "Two and Three Dimensional Unsteady Lift Problems in High Speed Flight," NACA Rept. 1077, 1952.

[19]Ballhaus, W. F. and Goorjian, P. M., "Computation of Unsteady Transsonic Flows by the Indicial Method," *AIAA Journal*, Vol. 15, Feb. 1978, pp. 117–124.

[20]Magnus, R. J., "Calculations of Some Unsteady Transsonic Flows about the NACA 64006 and 64A010 Airfoils," AFFDL-TR-77-46, July 1977.

[21]Mazelski, B., "Numerical Determination of Indicial Lift of a Two-Dimensional Sinking Airfoil at Subsonic Mach Numbers from Oscillatory Lift Coefficients with Calculations for a Mach Number of 0.7," NACA TN 2562, Dec. 1951.

[22]Mazelski, B. and Drischler, J. A., "Numerical Determination of Indicial Lift and Moment Functions of a Two-Dimensional Sinking and Pitching Airfoil at Mach Numbers of 0.5 and 0.6," NACA TN 2739, July 1952.

[23]Dowell, E. H., "A Simple Method for Converting Frequency Domain Aerodynamics into the Time Domain," NASA TM 81844, Oct. 1980.

[24]Jones, R. T., "The Unsteady Lift of a Wing of Finite Aspect Ratio," NACA Rept. 681, 1940.

[25]Dietze, F., "The Air Forces of the Harmonically Vibrating Wing in Compressible Medium at Subsonic Velocity (Plane Problem), Part II: Numerical Tables and Curves," Translation F-TS-948-RE, Air Material Command, U.S. Air Force, March 1947.

[26]Williams, M. H., "Unsteady Thin Airfoil Theory for Transsonic Flows with Embedded Shocks," *AIAA Journal*, Vol. 18, June 1980, pp. 615–624.

[27]Venkatesan, C. and Friedmann, P. P., "New Approach to Finite-State Modeling of Unsteady Aerodynamics," *AIAA Journal*, Vol. 24, Dec. 1986, pp. 1889–1897.

[28]Mazelski, B., "On the Noncirculatory Flow about a Two-Dimensional Airfoil at Subsonic Speeds," *Journal of the Aeronautical Sciences*, Dec. 1952, pp. 848–849.

[29]Leishman, J. G., "An Analytic Model For Unsteady Drag Below Stall," *Journal of Aircraft*, Vol. 25, July 1988, pp. 665–666.

[30]Woods, M. E., "Results from Oscillatory Pitch and Ramp Tests on the NACA 0012 Blade Section," Aircraft Research Association Memo 220, Bedford, England, 1979.

[31]Davis, S. S. and Malcolm, G. N., "Experimental Unsteady Aerodynamics of Conventional and Supercritical Airfoils," NASA TM 81221, Aug. 1980.

[32]Shampine, L. F. and Gordon, M. K., *Computer Solution of Ordinary Differential Equations—The Initial Value Problem*, W. H. Freeman and Co., San Francisco, 1975.

[33]Shampine, L. F., Watts, H. A., and Davenport, S. M., "Solving Nonstiff Ordinary Differential Equations—The State of the Art," *SIAM Review*, Vol. 18, July 1976, pp. 376–411.

[34]Grey, L. and Liiva, J., "Two-Dimensional Tests of Airfoils Oscillating Near Stall," USAAVLABS Technical Rept. 68–13B, Vol. II: Data Report, April 1968.

[35]Lorber, P. F. and Carta, F. O., "Unsteady Stall Penetration Experiments at High Reynolds Number," Rept. AFOSR TR-87-1202 and UTRC Rept. R87-956939-3, April 1987.

[36]Shamroth, S. J., and Geibling, H. J., "Analysis of Turbulent Flow About an Isolated Airfoil Using a Time-Dependent Navier-Stokes Procedure," AGARD CP 296, *Boundary Layer Effects on Unsteady Airloads*, 1980.